952 *Inorg. Chem.* **2010**, *49*, 952–959
DOI: 10.1021/ic901676e

Inorganic Chemistry
Article

Synthesis, Substitution Kinetics, and Electrochemistry of the First Tetrathiafulvalene-Containing β-Diketonato Complexes of Rhodium(I)

Eleanor Fourie,[†] Jannie C. Swarts,*[,†] Dominique Lorcy,[‡] and Nathalie Bellec[‡]

[†]*Department of Chemistry, University of the Free State, P.O. Box 339, Bloemfontein 9300, Republic of South Africa and* [‡]*Sciences Chimiques de Rennes, UMR 6226 CNRS-Université de Rennes 1, Matière Condensée et Systèmes Electroactifs (MaCSE), Campus de Beaulieu, Bât 10A, 35042 Rennes cedex, France*

Received August 22, 2009

The synthesis of the first rhodium(I) cyclooctadiene complexes containing tetrathiafulvalene (TTF) groups substituted on a β-diketonato ligand in either the methine position (3 position), [Rh(cod)($H_3CCOC\{S\text{-}TTF\text{-}(MeS)_3\}COCH_3$)] (**3**), or terminal position (1 position), [Rh(cod)$\{(Me_3\text{-}TTF)COCHCOCH_3\}$] (**4**), is reported. The effect of the β-diketonato substitution position on the kinetics of substitution of the TTF-containing β-diketonato ligand with 1,10-phenanthroline from **3** and **4** to give $[Rh(cod)(phen)]^+$, as well as on the electrochemical properties of **3** and **4**, was investigated. Second-order substitution rate constants, k_2, in methanol were found to be almost independent of the substitution position, with **4** ($k_2 = 2.09 \times 10^3$ dm^3 mol^{-1} s^{-1}) reacting only about twice as fast as **3**. An appreciable solvent pathway in the substitution mechanism was only observed for **4** with $k_s = 42$ s^{-1}. A complete mechanism for both substitution reactions is proposed. The electrochemistry of **3** and **4** in CH_2Cl_2/0.10 mol dm^{-3} $[N(^nBu)_4][B(C_6F_5)_4]$ showed three redox processes. Two of these were electrochemically reversible and are associated with the redox-active TTF group. For **3**, TTF-based formal reduction potentials, $E^{\circ\prime}$, were observed at 0.082 and 0.659 V vs Fc/Fc^+, respectively; **4** exhibited them at −0.172 and 0.703 V vs Fc/Fc^+ at a scan rate of 100 mV s^{-1}. A Rh^{II}/Rh^{I} redox couple was observed at $E^{\circ\prime} = 0.89$ V for **3**, after both TTF oxidations were completed, and at 0.51 V for **4**; this is between the two TTF redox processes. The more difficult oxidation of the Rh^I center of **3** indicates more effective electron-withdrawing from the Rh^I center to the first-oxidized TTF^+ group at the methine position of the β-diketonato ligand of $\mathbf{3}^+$ than to the terminal-substituted TTF^+ group in $\mathbf{4}^+$.

Introduction

Tetrathiafulvalene (TTF)-containing compounds possess unique electronic and magnetic properties, which caused them to be studied extensively as potential superconductors, charge-transfer complexes, ferromagnets, nonlinear optical materials, sensors, electroactive Langmuir−Blodgett films, and organic field-effect transistors.[1] Because of the high electron-donating ability of the reduced TTF group, recent studies have focused on the functionalization of this redox-active moiety, which can undergo two electrochemically reversible one-electron oxidations,[2] for use in coordination chemistry (Chart 1).[1−7]

Functional groups attached to the TTF core have ranged from amines[3] and phosphines[3] to β-diketonato[4] and carboxylato groups.[5] To date, only a few studies reported the

*To whom correspondence should be addressed. E-mail: swartsjc.sci@ufs.ac.za.

(1) (a) Lorcy, D.; Bellec, N. *Chem. Rev*. **2004**, *104*, 5185–5202. (b) Bellec, N.; Boubekeur, K.; Carlier, R.; Hapiot, P.; Lorcy, D.; Tallec, A. *J. Phys. Chem. A* **2000**, *104*, 9750–9759. (c) El-Wareth Sarhan, A.; Nouchi, Y.; Izumi, T. *Tetrahedron* **2003**, *59*, 6353–6362. (d) Cerveau, G.; Corriu, R. J. P.; Lerouge, F.; Bellec, N.; Lorcy, D.; Nobili, M. *Chem. Commun*. **2004**, 396–397. (e) Batail, P. *Chem. Rev*. **2004**, *104*, 4887 and the ensuing articles of this thematic issue on "Molecular Conductors". (f) El-Wareth, A. O.; Sarhan, A. *Tetrahedron* **2005**, *61*, 3889–3932. (g) Canevet, D.; Salle, M.; Zhang, G.; Zhub, D. *Chem. Commun*. **2009**, 2245–2269. (h) Naraso; Nishida, J.; Kumaki, D.; Tokito, S.; Yamashita, Y. *J. Am. Chem. Soc*. **2006**, *128*, 9598–9599.

(2) (a) Sezer, E.; Turksoy, F.; Tunca, U.; Ozturk, T. *J. Electroanal. Chem*. **2004**, *570*, 101–105. (b) Wu, J.-C.; Liu, S.-X.; Keene, T. D.; Neels, A.; Mereacre, V.; Powell, A. K.; Decurtins, S. *Inorg. Chem*. **2008**, *47*, 3452–3459. (c) Schnippering, M.; Zahn, A.; Liu, S.-X.; Leumann, C.; Decurtins, S.; Fermin, D. J. *Chem. Commun*. **2009**, 5552–5554.

(3) (a) Pellon, P.; Brulé, E.; Bellec, N.; Chamontin, K.; Lorcy, D. *J. Chem. Soc., Perkin Trans. 1* **2000**, 4409–4412. (b) Lorcy, D.; Bellec, N.; Fourmigué, M.; Avarvari, N. *Coord. Chem. Rev*. **2009**, *253*, 1398–1438.

(4) (a) Bellec, N.; Lorcy, D. *Tetrahedron Lett*. **2001**, *42*, 3189–3191. (b) Cosquer, G.; Pointillart, F.; Gal, Y. L.; Golhen, S.; Cador, O.; Ouahab, L. *Dalton Trans*. **2007**, 3495–3502. (c) Xu, C.-H.; Sun, W.; Zhang, C.; Zhou, C.; Fang, C.-J.; Yan, C.-H. *Chem.—Eur. J*. **2009**, *15*, 8717–8721.

(5) Gu, J.; Zhu, Q.; Zhang, Y.; Lu, W.; Niu, G.; Dai, J. *Inorg. Chem. Commun*. **2008**, *11*, 175–178.

(6) (a) Massue, J.; Bellec, N.; Chopin, S.; Levillain, E.; Roisnel, T.; Clérac, R.; Lorcy, D. *Inorg. Chem*. **2005**, *44*, 8740–8748. (b) Bellec, N.; Massue, J.; Roisnel, T.; Lorcy, D. *Inorg. Chem. Commun*. **2007**, *10*, 1172–1176.

(7) (a) Zhu, Q.; Bian, G.; Zhang, Y.; Dai, J.; Zhang, D.; Lu, W. *Inorg. Chim. Acta* **2006**, *359*, 2303–2308. (b) Li, Y.-J.; Liu, W.; Li, Y.-Z.; Zuo, J.-L.; You, X.-Z. *Inorg. Chem. Commun*. **2008**, *11*, 1466–1469. (c) Zheng, P.; Guo, Y.-J.; Liu, W.; Li, Y.-Z.; Zuo, J.-L.; You, X.-Z. *Transition Met. Chem*. **2008**, *33*, 767–773.

 Published on Web 01/04/2010

Chart 1. Redox Processes of the TTF Core

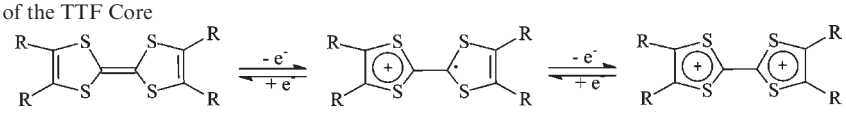

coordination of these TTF-containing β-diketonato ligands complexed to metal centers. The first studies focused on bis-(tetrathiafulvalenyl)acetonato complexes of nickel, zinc, and copper having the general formula [M(TTF-β-diketonato)$_2$(pyridine)$_2$].[6] Others reported on square-planar manganese and copper complexes [M(TTF-β-diketonato)$_2$].[7] More recently, octahedral complexes of tetrathiafulvalene carboxylates with cobalt and nickel have also been reported.[5] In this paper, we report the first rhodium-containing tetrathiafulvalenyl-β-diketonato complexes, [Rh(cod)(TTF-β-diketonato)], investigate the kinetics of β-diketonato substitution with 1,10-phenanthroline (phen), and relate the kinetic results to the electrochemical properties of these complexes as determined by cyclic voltammetry (CV). These new complexes may show anticancer activity, similar to the [Rh(cod)-(acac)] complexes previously described by Sava and coworkers.[8]

[Rh(cod)(β-diketonato)] complexes can undergo substitution to replace either of the two ligands, as shown in Scheme 1, depending on the nature of the incoming ligand. In the case of strong σ-donating incoming ligands, such as phen and 2,2′-bipyridyl, the σ-donating β-diketonato ligand is substituted.[9] If the incoming ligand has π-bonding capability, such as phosphites, the π-bonding cod ligand is replaced.[10]

For β-diketonato substitution, the rate of substitution is dependent on the group electronegativity, χ_R, of the β-diketonato side groups.[9] An increase in the value of χ_R on the Gordy scale of R substituents of $(R^1COCHCOR^2)^-$ lowers the electron density on the rhodium center and also increases the rate of substitution. Gordy-scale χ_R values are empirical numbers that express the combined tendency of not only one atom but also a group of atoms like CF_3 to attract electrons (including those in a covalent bond) as a function of the number of valence electrons, n, and the covalent radius, r (in Å), of groups as discussed elsewhere.[11] However, the rate of β-diketonato substitution becomes almost independent of the β-diketonato substituent group electronegativity if the substituent becomes strongly electron-donating. It was also shown that an increase in the pK_a of the free β-diketone ligand decreases the β-diketonato substitution rate; the pK_a and terminal β-diketonato substituent group electronegativities, χ_{R1} and χ_{R2}, are related to the equation pK_a = $-3.484(\chi_{R1} + \chi_{R2}) + 24.6$.[12]

Substitution of the β-diketonato group on [Rh(cod)(β-diketonato)] complexes by incoming NN ligands like phen usually takes place via an associative mechanism, which is characterized by a large negative entropy of activation ($\Delta S^{\ddagger}$) and a negative volume of activation ($\Delta V^{\ddagger}$).[9,13] A neutral five-coordinate 18-electron intermediate species of the type [Rh(β-diketonato)(cod)(NN)], where only one of the N atoms of the incoming NN ligand is coordinated, is first formed. The rate-determining step is thought to be bond breakage of the Rh−O bond closest to the more electronegative β-diketonato substituent.[14]

Results and Discussion

Complex Synthesis, Group Electronegativities, and pK_a Values. β-Diketones substituted with the TTF-containing group in either the methine, **1**, or the terminal position, **2**, were reacted as shown in Scheme 2 with [$Rh_2Cl_2(cod)_2$)] in *N*,*N*-dimethylformamide (DMF) to give **3** and **4** as brown and dark-red solids, respectively, in high (> 70%) yield. Complexes are stable in air and can be stored for long periods of time (> 1 year) without degradation. The group electronegativity of the Me_3-TTF group of **2**, $\chi_{Me_3\text{-TTF}}$ = 2.01, was obtained from the carbonyl IR stretching frequency, ν(C=O) = 1710 cm^{-1}, of the methyl ester Me_3-TTF-COOMe, utilizing the equation[15] ν(C=O) = $74.543\chi_R + 1560.5$. This makes Me_3-TTF one of the more electron-donating groups so far studied. To put it into perspective, χ_{CH_3} = 2.34, while χ_{CF3} = 3.01. The strongly electron-donating ferrocenyl group with χ_{Fc} = 1.87 is just slightly more electron-donating than the Me_3-TTF group.[15] From the $\chi_{Me_3\text{-TTF}}$ and χ_{CH_3} values, the pK_a of **2**, (Me_3-TTF)-$COCH_2COCH_3$, could be estimated as 9.44, utilizing the equation[12] pK_a = $-3.484(\chi_{R1} + \chi_{R2}) + 24.6$.

UV/Vis Spectroscopy. The UV/vis spectra of **3** and **4** and the reaction mixture containing the substituted product [Rh(cod)(phen)]$^+$, free **1**$^-$, and a 50-fold excess of phen after **3** reacted with phen are shown in Figure 1. The UV/vis spectrum of the pure product [Rh(cod)(phen)]$^+$ with λ_{max} (ε/dm^3 mol^{-1} cm^{-1} values in brackets) at 457 nm (810) and $\lambda_{shoulder}$ = 367 nm (4620) is presented elsewhere.[15a] A linear relationship between the absorbance and concentration was observed for both **3** and **4**, confirming the validity of the Beer−Lambert law $A = \varepsilon Cl$, where l = path length, for both of these complexes at the wavelength selected for kinetic studies. Molar extinction coefficients, ε, in units of dm^3 mol^{-1} cm^{-1} at the experimental wavelengths where substitution was monitored were 7950 ± 10 (λ_{exp} = 320) for **3** and 1860 ± 10 (490 nm) for **4**. Other important extinction coefficients were found to be 2015 ± 10 dm^3 mol^{-1} cm^{-1} at λ_{max} = 418 nm for **3** and 2088 ± 10 dm^3 mol^{-1} cm^{-1} at λ_{max} = 424 nm for **4**.

(8) (a) Giraldi, T.; Sava, G.; Bertoli, G.; Mestroni, G.; Zassinovich, G. *Cancer Res.* **1977**, *37*, 2662–2666. (b) Sava, G.; Zorzet, S.; Perissen, L.; Mestroni, G.; Zassinovich, G.; Bontempi, A. *Inorg. Chim. Acta* **1987**, *137*, 69–71.

(9) Vosloo, T. G.; du Plessis, W. C.; Swarts, J. C. *Inorg. Chim. Acta* **2002**, *331*, 188–193.

(10) Leipoldt, J. G.; Lamprecht, G. J.; Steynberg, E. C. *J. Organomet. Chem.* **1990**, *397*, 239–244.

(11) (a) Wells, P. R. *Progress in Physical Organic Chemistry*; John Wiley & Sons, Inc.: New York, 1968; Vol. *6*, p 111. (b) Kagarise, R. E. *J. Am. Chem. Soc.* **1955**, *77*, 1377–1379.

(12) Conradie, J.; Swarts, J. C. *Organometallics* **2009**, *28*, 1018–1026.

(13) Leading references discussing negative $\Delta V^{\ddagger}$ values for an associative mechanism include the following: (a) Leipoldt, J. G.; Steynberg, E. C.; van Eldik, R. *Inorg. Chem.* **1987**, *26*, 3068–3070. (b) House, J. E. *Principles of Chemical Kinetics*; William C. Brown Publishers: Dubuque, IA, 1997; p 75.

(14) Vosloo, T. G.; Swarts., J. C. *Transition Met. Chem.* **2002**, *27*, 411–415.

(15) (a) Du Plessis, W. C.; Vosloo, T. G.; Swarts, J. C. *Dalton Trans.* **1998**, 2507–2514. (b) Du Plessis, W. C.; Erasmus, J. J. C.; Lamprecht, G. J.; Conradie, J.; Cameron, T. S.; Aquino, M. A. S.; Swarts, J. C. *Can. J. Chem.* **1999**, *77*, 378–386.

Scheme 1. Substitution Reactions of [Rh(cod)(β-diketonato)] Complexes

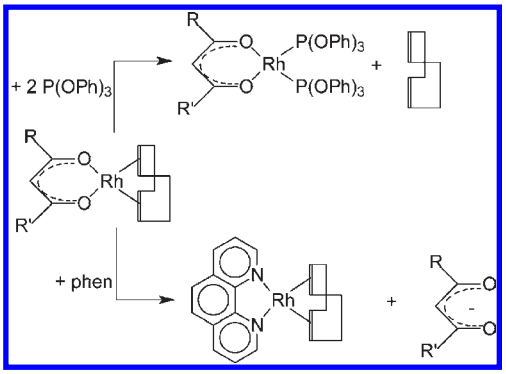

Scheme 2. Synthesis of Rhodium(I) Complexes with TTF-Containing β-Diketonato Ligands

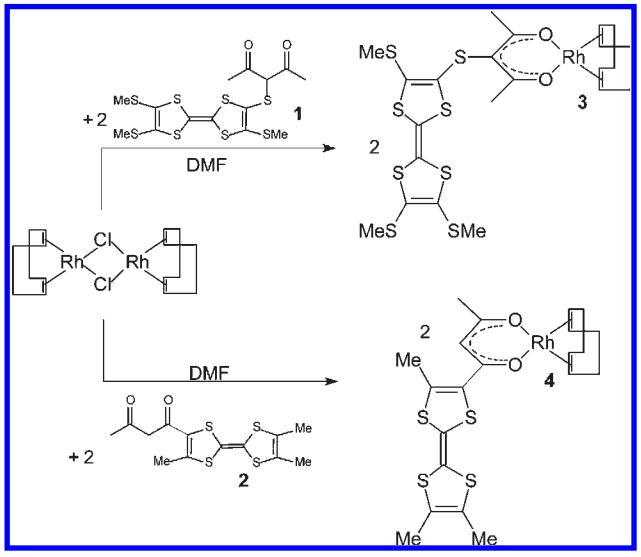

Kinetics. The substitution reaction of the rhodium complexes **3** and **4** with phen in methanol as the solvent proceeds with the replacement of the β-diketonato ligand to form $[Rh(cod)(phen)]^+$. The dependence of pseudo-first-order rate constants, k_{obs}, on phen concentrations for **3** and **4** is shown in Figure 2 (left), the slope of which gave second-order rate constants, k_2. The intercepts gave the first-order rate constant associated with a solvent pathway, k_s. Second-order rate constants obtained from a reaction temperature variation between 5 and 41 °C were used to determine the activation parameters $\Delta H^{\ddagger}$ and $\Delta S^{\ddagger}$ graphically, according to the Eyring equation, eq 2, as shown in Figure 2.

The results are summarized in Table 1. Large second-order rate constants were obtained for both compounds, with **4** having a second-order rate constant approximately double that of **3**. This difference in k_2 is not significant and indicates that the substitution position of a bulky TTF group has a relatively small influence on the rate of substitution reactions. However, in the case of **4**, the $(Me)_3$-TTF side group is a terminal substituent directly linked with the pseudoaromatic core of the β-diketonato ligand. Conjugation between the TTF group and the pseudoaromatic β-diketonato core will limit the rotation of the TTF group much, rendering it unlikely to interfere

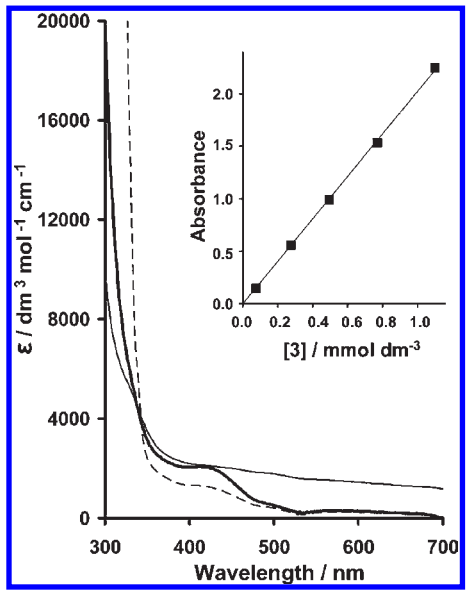

Figure 1. UV/vis spectra of **3** (bold line), **4** (solid line), and $[Rh(cod)(phen)]^+$ (dashed line) in methanol at 25 °C. Inset: Linear Beer−Lambert law relationship between the absorbance and concentration for **3** at λ_{max} = 418 nm.

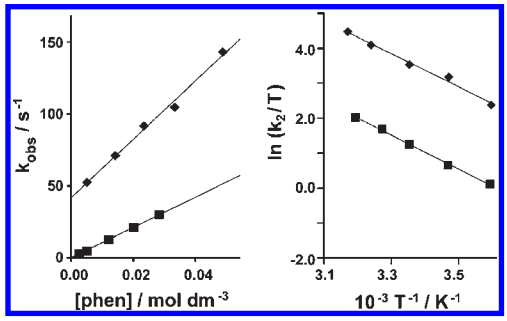

Figure 2. Left: Linear relationship between pseudo-first-order rate constants (k_{obs}) and the phen concentration for β-diketonato substitution from **3** (■) and **4** (♦) with phen at 25 °C, which gave second-order rate constants, k_2, as the slope. Right: Eyring plot of $\ln(k_2/T)$ vs T^{-1} for **3** (■) and **4** (♦), measured at temperatures ranging from 5 to 41 °C.

with approaching pathways of attacking nucleophiles on the Rh^I center. In the case of **3**, the $(MeS)_3$-TTF-S group is at the β-diketonato 3 position (the methine position), but the sulfur spacer breaks conjugation between it and the pseudoaromatic β-diketonato core. This would allow free rotation of the sulfur as well as the $(MeS)_3$-TTF group and allow the latter to have more steric interference with rhodium-attacking incoming nucleophiles, a conclusion that is consistent with **3** undergoing β-diketonato substitution slightly more slowly than **4**.

Strikingly, the reactivity relationships of Figure 2 show for derivative **3** a zero intercept, while for **4**, a nonzero intercept of $k_s = 42\ s^{-1}$ was obtained. This implies that for **4** a solvent pathway in addition to direct substitution makes a significant contribution to the substitution mechanism. This observation has been observed in only a few other cases for [Rh(cod)(β-diketonato)] complexes[9] and usually is associated with β-diketonato ligands having phenyl substituents. The likelihood of a bidentate ligand like β-diketones being replaced by a monodentate solvent molecule, here methanol, is low. Hence, the rate constants associated with a solvent path, k_s values, are

Table 1. Second-Order Substitution Rate Constants, k_2, First-Order Solvent Path Rate Constants, k_s, as Well as Activation Parameters for Substitution Reactions Spectroscopically Measured by the Stopped-Flow Technique at the Indicated Wavelengths

compound	λ_{exp}/nm	k_2/dm^3 mol^{-1} s^{-1}	k_s/s^{-1}	$\Delta H^{\ddagger}$/ kJ mol^{-1}	$\Delta S^{\ddagger}$/ J K^{-1} mol^{-1}
3	320	1050(10)	0	39.2(3)	−36.2(1)
4	490	2030(90)	42(3)	40.6(5)	−51.1(1)

usually small compared to the direct second-order substitution rate constant k_2. For the present study involving **4**, k_s is unusually large. It shows that even at phen concentrations as high as 0.024 mol dm^{-3} (a 300-fold excess over **4** giving rise to $k_{obs} = 82$ s^{-1}), still more than half of the substituted product, [Rh(cod)(phen)]$^+$, is generated via the solvent pathway.

From the slope and y intercept of the Eyring plot (Figure 2, right), $\Delta S^{\ddagger}$ and $\Delta H^{\ddagger}$ (Table 1) were determined by utilizing eq 2; see the Experimental Section. A large negative $\Delta S^{\ddagger}$ value (typically[9,13] $\Delta S^{\ddagger} < -80$ J K^{-1} mol^{-1} for [Rh(cod)(β-diketonato)] complexes) is consistent with the substitution reaction proceeding via an associative mechanism. Although the $\Delta S^{\ddagger}$ values of both **3** and **4** are about half this, they still are substantially negative values and as such indicate that β-diketonato substitution predominantly must take place via an associative mechanism. It has been shown elsewhere that β-diketonato substitution in [Rh(cod)(β-diketonato)] complexes with phenanthroline derivatives having $3.03 < pK_a < 6.31$ are independent of the phen derivative pK_a.[14] pK_a of phen is 4.86.[14] Substitution is, however, dependent on pK_a of the leaving β-diketonato ligand.[9] It was concluded that Rh−N bond formation is not the rate-determining step but rather the Rh−O bond breakage is.[14] Furthermore, the results from this earlier study were consistent with the Rh−O bond adjacent to the more electron-withdrawing terminal β-diketonato substituent breaking first.[14] When these principles are applied to **3** and **4** in the direct substitution path, it is proposed that phenanthroline first associates via one of its N atoms in a fast equilibrium with **3** or **4**, thereby forming a 18-electron five-coordinate species. The rate-determining step then follows and consists of the near simultaneous breaking of the β-diketonato Rh−O bond adjacent to the most electron-withdrawing terminal β-diketonato substituent, followed by strong bond formation between the second phenanthroline N atom and the rhodium center to give a new five-coordinated transition species. This new intermediate quickly dissociates to liberate the β-diketonato anion and form [Rh(cod)(phen)]$^+$ as the product. The initial O−Rh bond breakage occurs at the O atom next to the CH_3 group in **4** because $\chi_{CH_3} = 2.34$ is larger than $\chi_{Me_3\text{-}TTF} = 2.01$ and indicates that the CH_3 group is more electron-withdrawing. For **3**, oxygen bond breakage can occur at either of the two equivalent O atoms because of its symmetric substitution pattern.

Scheme 3 provides a schematic presentation of this mechanism. The structures shown are not intended to indicate absolute geometries. Rather, they indicate possible coordination modes of transition states. Also shown in Scheme 3 is a possible mechanism to highlight the solvent path of substitution exhibited by **4** only.

The key difference between the reactivity properties of **3** and **4** to allow **4** to exhibit a substantial contributing solvent route in the mechanism while **3** does not relates to the size of the equilibrium constant, K (Scheme 3), in the equilibrium between the rhodium complex and the solvent, here methanol. The equilibrium position between methanol and **3** must be far to the left, implying a small K, to exclude detection of the solvent path. This means phen will be free to coordinate unhindered with **3** according to the direct substitution route. For **4**, the value of K is such that, at the concentrations of **4** used, the equilibrium is shifted sufficiently to the right to allow for noticeable amounts of **4** and **4-MeOH** to exist simultaneously in solution. Provided the equilibrium between **4** and the solvent is fast and that the reactivities of **4-MeOH** and **4-phen** are not too different, simultaneous observation of the solvent and direct routes of β-diketonato substitution from **4** would be possible.

Electrochemistry. The electrochemistries of rhodium complexes **3** and **4**, as well as TTF-containing β-diketonato ligands **1** and **2**, were investigated in CH_2Cl_2/0.1 mol dm^{-3} [N^{n}Bu$_4$][B(C$_6$F$_5$)$_4$] as the solvent and supporting electrolyte. Cyclic voltammograms of uncoordinated ligands **1** and **2** showed two one-electron-transfer redox couples associated with the TTF core; these are labeled as 1 and 2 in Figure 3. Electrochemical data are summarized in Table 2. Wave 1 was observed at $E^{\circ\prime}$ values of +22 and −111 mV vs Fc/Fc$^+$ for **1** and **2**, respectively, and is associated with the formation of **1**$^+$ and **2**$^+$. $E^{\circ\prime}$ values for wave 2 were at 630 and 677 mV, respectively, and are associated with the formation of the double-oxidized species **1**$^{2+}$ and **2**$^{2+}$. $\Delta E_p = E_{pa} - E_{pc}$ values of smaller than 90 mV were observed for waves 1 and 2, at scan rates of 100 mV s^{-1}, indicating that the processes approach electrochemical reversibility (Table 2) at slow scan rates. The theoretical ΔE value of one-electron-transfer electrochemically reversible processes is 59 mV.[16] In addition, a plot of i_{pa} versus the square root of the scan rate deviated only slightly from linearity at high scan rates; see the Supporting Information. This is consistent with good electrochemical reversibility,[2c,16] especially at slow scan rates. Both compounds **1** and **2** showed peak current ratios approaching 1. Linear sweep voltammetry (LSV; Figure 3) indicated that an equal number of electrons, namely, one,[1,2] are associated with waves 1 and 2. It was found that $\Delta E^{\circ\prime} = E^{\circ\prime}_{wave\ 2} - E^{\circ\prime}_{wave\ 1} = 608$ mV for **1** but 788 mV for **2**. This clearly shows that **2** is more efficient in delocalizing the charge in charged intermediates like **2**$^+$ than **1** is at delocalizing the charge in intermediates such as **1**$^+$, because of the absence of a spacer atom between the TTF group and the β-diketonato pseudoaromatic core in **2** compared **1**. $\Delta E^{\circ\prime} = 0.788$ V for **2** clearly highlights differences between studies utilizing [N^{n}Bu$_4$][B(C$_6$F$_5$)$_4$] as the supporting electrolyte rather than [N^{n}Bu$_4$][PF$_6$], which gave $\Delta E^{\circ\prime} = 0.5$ V, as described in a preliminary report by one of us on the electrochemistry for **2** only.[6b] The reason for this difference can be

(16) (a) Evans, D. H.; O'Connell, K. M.; Peterson, R. A.; Kelly., M. J. *J. Chem. Educ.* **1983**, *60*, 290–293. (b) Kissinger, P. T.; Heineman, W. R. *J. Chem. Educ.* **1983**, *60*, 702–706. (c) Van Benshoten, J. J.; Lewis, J. Y.; Heineman, W. R. *J. Chem. Educ.* **1983**, *60*, 772–776. (d) Mobbott, G. A. *J. Chem. Educ.* **1983**, *60*, 697–702.

Scheme 3. Possible Associative Mechanism of β-Diketonato Substitution from [Rh(TTF-β-diktonato)(cod)] Complexes with phen[a]

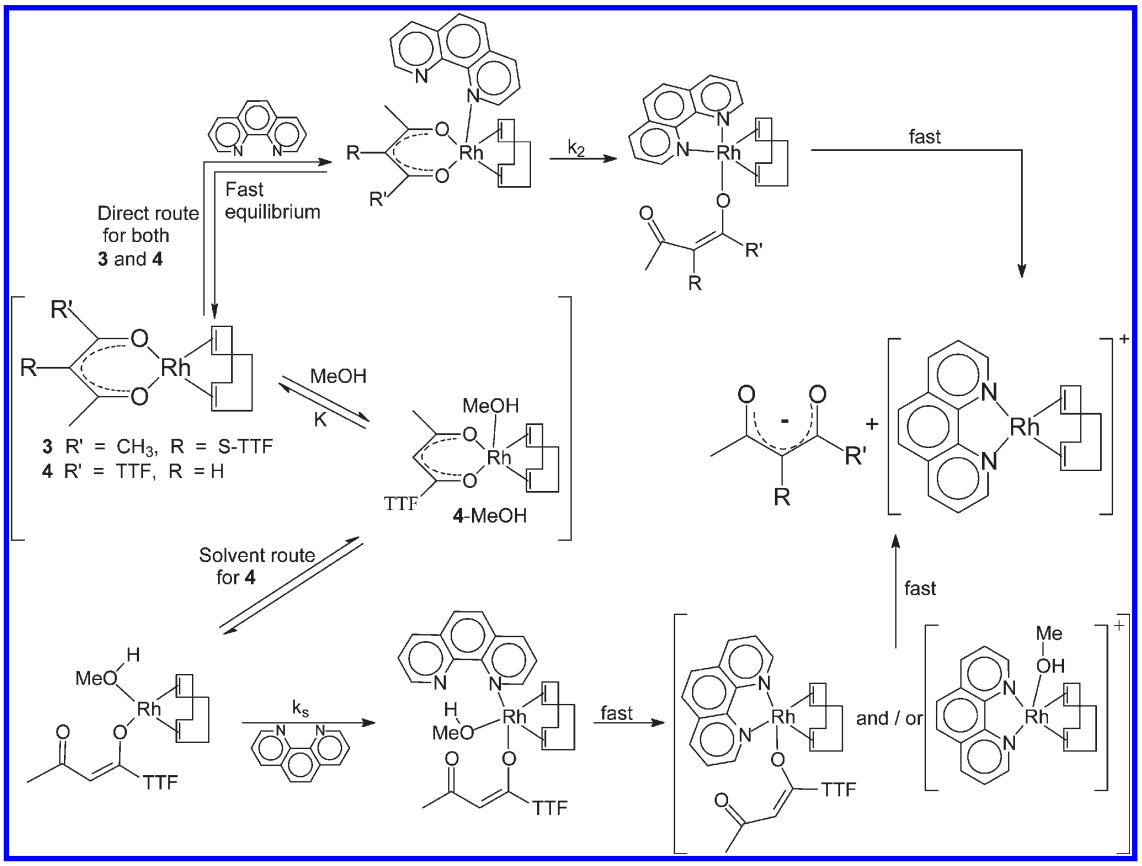

[a] The direct k_2 route is valid for both **3** and **4**, while the solvent k_s route (bottom) is only valid for **4**. Here, TTF really denotes $(Me)_3$-TTF, while S-TTF = $(MeS)_3$-TTF-S; TTF = tetrathiafulvalenyl. Full structures of **3** and **4** are given in Scheme 2.

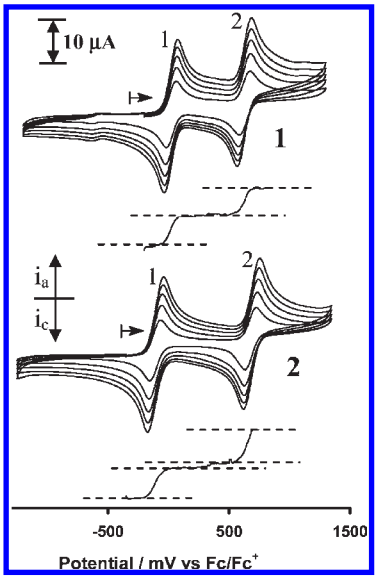

Figure 3. Cyclic voltammograms at scan rates of 100 (smallest peak current), 200, 300, 400, and 500 mV s^{-1} and LSVs at 2 mV s^{-1} of free TTF-containing β-diketone ligands **1** and **2** in CH_2Cl_2/0.1 mol dm^{-3} [N(^{n}Bu$_4$)][B(C_6F_5)], T = 25 °C, on a glassy carbon working electrode.

traced to the negative charge of the anion $[B(C_6F_5)_4]^-$, which is distributed over a much larger volume than $[PF_6]^-$. This means that $[B(C_6F_5)_4]^-$ will interact much weaker with $\mathbf{2}^+$ or $\mathbf{2}^{2+}$ to form ion pairs. This observation is in agreement with other findings that also indicate that the results obtained in $[B(C_6F_5)_4]^-$ media are frequently a more true reflection of the electrochemical fingerprints of positively charged oxidized species.[17]

The 22 − (−111) = 133 mV lowering of $E^{o\prime}_{wave\ 1}$ in moving from **1** to **2** is substantial, and it shows that **2** is more electron-rich than **1**. This difference is, in part, a consequence of the Me_3-TTF group of **2** delocalizing electrons from the electron-withdrawing β-diketonato core better from the terminal position than the $(MeS)_3$-TTF-S group of **1** delocalizing it from the methine position via an S spacer atom, but probably the combined electronic effect of four S atoms attached to the $(MeS)_3$-TTF-S group of **2** has the biggest influence in raising the formal reduction potential of **1** with 133 mV. This large difference in the formal reduction potential between **1** and **2** also contrasts the small increase in the rate of substitution in moving from **3** to **4**.

The electrochemistries of rhodium(I) tetrathiafulvalene complexes **3** and **4** are shown in Figure 4; data are summarized in Table 2. Each complex showed two redox couples belonging to the TTF core, as well as a rhodium redox couple. In the case of **3**, waves 1 and 2 are associated

(17) For leading references demonstrating how the use of [N^{n}Bu$_4$][B(C_6F_5)$_4$] and/or [N^{n}Bu$_4$][B($C_6H_3(CF_3)_2$)$_4$] as the supporting electrolyte can lead to enhanced electrochemical interpretations, see:(a) Barriere, F.; Camire, N.; Geiger, W. E.; Mueller-Westerhoff, U. T.; Sanders, R. *J. Am. Chem. Soc.* **2002**, *124*, 7262–7263. (b) Barriere, F.; Geiger, W. E. *J. Am. Chem. Soc.* **2006**, *128*, 3980–3989. (c) Kemp, K. C.; Fourie, E.; Conradie, J.; Swarts, J. C. *Organometallics* **2008**, *27*, 357–362. (d) Swarts, J. C.; Nafady, A.; Roudebush, J. H.; Trupia, S.; Geiger, W. E. *Inorg. Chem.* **2009**, *48*, 2156–2165.

Table 2. Electrochemical Data[a] at a Scan Rate of 100 mV s^{-1} (Potentials in mV vs Fc/Fc^+) Obtained for TTF-Containing Compounds **1**−**4** in CH_2Cl_2/0.1 mol dm^{-3} $[NBu_4][B(C_6F_5)]$, at 25 °C

compound	E_{pa}/mV	ΔE_p/mV	$E^{\circ\prime}$/mV	i_{pa}/μA	i_{pc}/i_{pa}
Fc*, Fc[b]	−573, 37	68, 75	−607, 0	4.54, 5.65	0.99, 0.98
1	64 (675)	84 (90)	22 (630)	5.79 (5.36)	0.97 (0.96)
2	−68 (723)	86 (92)	−111 (677)	7.46 (7.23)	0.99 (0.98)
3	151 (726) [931]	139 (134) [86]	82 (659) [888]	1.68 (1.75) [0.30]	0.95 (0.96) [0.80]
4	−136 (746) [555]	88 (86) [90]	−172 (703) [510]	6.48 (4.85) [5.25]	0.95 (0.94) [0.34]

[a] For **1**−**4**, data for the first TTF redox processes are presented first, while those of the second TTF redox process are presented in round brackets. Data for the rhodium-based process of **3** (wave 3) and **4** (wave 2) are presented in square brackets. [b] The first values are data applicable to decamethylferrocene, Fc*; the second values are data applicable to ferrocene, Fc.

with electrochemical quasi-reversible one-electron-transfer processes at $E^{\circ\prime} = 0.08$ and 0.66 V vs Fc/Fc^+; ΔE_p values are ca. 140 and 90 mV at 100 mV s^{-1} for **3** and **4**, respectively. Peak current ratios approached 1. Oxidation of the rhodium center from Rh^I to Rh^{II} in a one-electron-transfer process (see the LSV in Figure 4) was observed at 0.89 V (wave 3) for **3**, with ΔE_p values between 86 and 134 mV depending on the scan rate. This indicated that electrochemical reversibility was only maintained at slow scan rates. The rhodium redox couple was not chemically reversible on the CV time scale; peak current ratios of smaller than 0.8 were observed and are consistent with the instability of Rh^{II} complexes. A characteristic property of **3** is that both TTF-based electron-transfer processes are completed *before* the rhodium center is oxidized. As the scan rate is increased from 100 to 500 mV s^{-1}, a decrease is observed in the peak current ratios i_{pc}/i_{pa} of the rhodium redox couple, wave 3. However, because of the uncertainty and inaccuracy of the measured wave 3 currents, which is considered a consequence of the slow electrochemical rate of Rh^I oxidation, leading to poor peak resolution, this drift in the current ratio cannot be interpreted. Strikingly though, despite the peak broadening of wave 3 as a result of slow electron transfer (i.e., irreversible thermodynamics disobeying the Nernst equation), which made i_p values difficult to measure or even observe, LSV still counted relatively accurately that one electron was transferred during this process, the same amount as that for the TTF-based electron-transfer steps. The square-wave voltammogram of **3** (Figure 4) made observation of the Rh-based redox process associated with wave 3 easier to observe than CV did and accentuated the peak broadening that is associated with this process.

Complex **4** also showed three one-electron-transfer processes. Wave 1 represents an electrochemically reversible one-electron redox couple associated with the TTF core, at $E^{\circ\prime}_{\text{wave 1}} = -0.17$ V having $\Delta E_p \approx 90$ mV at scan rates of 100−500 mV s^{-1}. Wave 3 represents the second TTF one-electron-transfer process at $E^{\circ\prime}_{\text{wave 3}} = 0.70$ V and a ΔE_p value of ca. 90 at slow (100 mV s^{-1}) scan rates. At faster scan rates, ΔE_p became progressively larger, with a value of 130 mV s^{-1} being observed at 500 mV s^{-1}.

Peak current ratios were found to be approaching 1. In contrast with complex **3**, oxidation of the Rh^I center in a one-electron-transfer process to give a rhodium(II) species for **4** was observed at 0.51 V, wave 2, *between* the TTF processes and not after them. Thus, oxidation of Rh^I occurred 380 mV lower for **4** than for **3**. ΔE_p values between 90 and 130 mV indicated electrochemical reversibility for this rhodium-based redox process at slow scan rates. Electrochemical reversibility for the electron-transfer processes of **3** and **4** at slow scan rates was also confirmed by plots of i_{pa} versus the square root of the scan rate; see the Supporting Information. The rhodium redox couple was not chemically reversible; peak current ratios of smaller than 0.5 were observed. This is consistent with slow rhodium(II) decomposition. Decomposition here probably included the formation of an unidentified rhodium-(III) complex. On the reverse scan, a broad reduction wave was observed at ca. −1090 mV, wave 4 (Figure 4). This peak is so broadened that it is more identifiable at faster

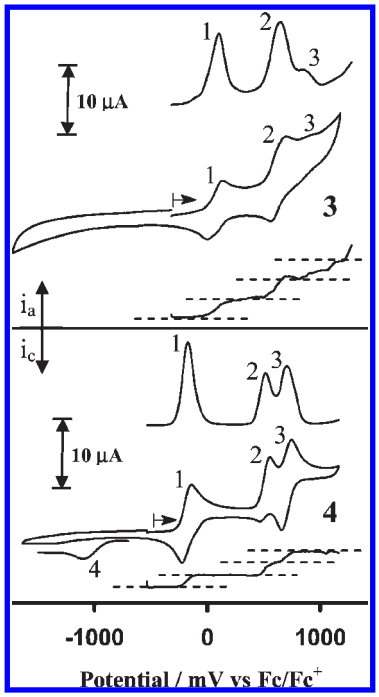

Figure 4. Cyclic voltammograms of TTF-containing rhodium(I) complexes **3** and **4**, at a scan rate of 100 mV s^{-1}, in CH_2Cl_2/0.1 mol dm^{-3} $[N(^nBu_4)][B(C_6F_5)]$, $T = 25$ °C, on a glassy carbon working electrode. Square waves (top of each figure) at a frequency of 10 Hz, as well as LSVs at 2 mV s^{-1} (bottom of each figure), are also shown for each complex. Inset for **4**: Peak 4 is an overlay of a Rh^{III} reduction peak at 500 mV s^{-1}.

(18) The rhodium(III) complex $[Rh(FcCOCHCOCF_3)(CH_3)(I)(CO)(PPh_3)]$ was recently synthesized and characterized. See: Conradie J.; Swarts, J. C. *Organometallics* **2009**, *28*, 1018−1026. A detailed electrochemical study on this complex showed that a reduction of the Rh^{III} center occurred at −1.492 mV vs Fc/Fc^+ in CH_2Cl_2 containing 0.10 mol dm^{-3} $[N(^nBu)_4][PF_6]$ as the supporting electrolyte. The manuscript of this study is currently in preparation (Conradie, J.; Swarts, J. C. *Organometallics*, to be submitted). Further, a Rh^{III} reduction of an electrochemically generated Rh^{III} species in $[Rh(FcCOCHCOR)(CO)_2]$ complexes (R = CF_3, Ph, CH_3, and Fc) was also observed between −0.687 and −1.187 mV, depending on the R group. See:Conradie, J.; Cameron, T. S.; Aquino, M. A. S.; Lamprecht, G. J.; Swarts, J. C. *Inorg. Chim. Acta* **2005**, *358*, 2530−2542.

scan rates. Wave 4 is not observed if the reversal potential of the forward anodic sweep is set to exclude wave 2 but is observed if the reversal potential is set to include the rhodium-based process of wave 2 but exclude wave 3. In analogy to the results of other electrochemical studies, this cathodic wave is probably associated with the reduction of a decomposition rhodium(III) species.[18] Complex **3** did not show a similar wave at large negative potentials.

LSVs of both complexes **3** and **4** show the number of electrons involved to be equal for waves 1−3. On the basis of the proven one-electron-transfer processes of TTF,[1,2] this confirms all three processes to be one-electron-transfer processes, giving further proof for the one-electron oxidation of Rh^{I} to Rh^{II}. The electrochemical schemes below highlight the different electrochemical behavior of **3** and **4**.

$$\text{For } \mathbf{3}: \quad [(TTF)Rh^{I}] \overset{E^{o\prime} = 82\ mV}{\rightleftharpoons} [(TTF^{+})Rh^{I}] \overset{E^{o\prime} = 659\ mV}{\rightleftharpoons} [(TTF^{2+})Rh^{I}] \overset{E^{o\prime} = 888\ mV}{\rightleftharpoons} [(TTF^{2+})Rh^{II}]$$

$$\text{For } \mathbf{4}: \quad [(TTF)Rh^{I}] \overset{E^{o\prime} = -172\ mV}{\rightleftharpoons} [(TTF^{+})Rh^{I}] \overset{E^{o\prime} = 510\ mV}{\rightleftharpoons} [(TTF^{2+})Rh^{II}] \overset{E^{o\prime} = 703\ mV}{\rightleftharpoons} [(TTF^{2+})Rh^{II}]$$

The ease by which Rh^{I} can be oxidized to Rh^{II} in $\mathbf{4}^{+}$ at 0.51 V, i.e., before the TTF group has been oxidized for the second time, as compared to $\mathbf{3}^{2+}$ at 0.89 V (after both TTF oxidations occurred during the anodic scan) indicates that the rhodium center of $\mathbf{3}^{+}$ is more electron-poor than that of $\mathbf{4}^{+}$. The electrophilic properties of the first oxidized state of the tetrathiafulvenyl group, TTF^{+}, are thus clearly better relayed to the Rh center of $\mathbf{3}^{+}$ than of $\mathbf{4}^{+}$. This cannot be due to better conjugation between the pseudoaromatic β-diketonato core and the oxidized TTF group in $\mathbf{3}^{+}$ because the TTF group of **3** is separated from the β-diketonato core by an S spacer atom. This means that the substituent position of 3 at the methine position is more effective in relaying its electron-withdrawing properties probably as a through-space field effect[19] to the rhodium center.

Conclusion

This study described the first synthesis of rhodium(I) complexes [Rh(β-diketonato)(cod)] **3** and **4** coordinated to TTF-sustituted β-diketonato ligands **1** and **2**. Complexes **3** and **4** differed by having the TTF group substituted either at the terminal position of the β-diketonato ligand or at the methine position, i.e., between the two β-diketonato carbonyl groups. It was shown that substitution of the β-diketonato ligand in [Rh(β-diketonato)(cod)] with phen proceeds via an associative mechanism. In view of the large difference in the formal reduction potentials of the Rh^{I} center, 890 mV vs Fc/Fc^{+} for **3** and 510 mV for **4**, it was surprising to observe that the different TTF substitution positions of **3** and **4** have such a small influence on the kinetics of β-diketonato substitution. The rate of the substitution reaction only increased from 1080 to 2030 $dm^{3}\ mol^{-1}\ s^{-1}$ in moving from **3** to **4**. An unusually large solvent-induced substitution pathway was observed with **4**. This relates to the higher nucleophilic character of the Rh^{I} center in **4** as identified by the low formal reduction potential of Rh^{I} oxidation in this complex. This also caused the second TTF oxidation step of **4** to occur after Rh^{I} oxidation, while in **3**, both TTF one-electron oxidations occurred before Rh^{I} oxidation. For both **3** and **4**, the one-electron-transfer TTF redox steps were electrochemically reversible at slower scan rates, but the one-electron oxidation of Rh^{I} to a Rh^{II} species showed only partial electrochemical and chemical reversibility.

Experimental Section

General Information. $[Rh_2Cl_2(cod)_2]$,[20] **1**,[6a] **2**,[6b] and tetrabutylammonium tetrakis(pentafluorophenyl)borate, $[N(^{n}Bu)_4][B(C_6F_5)_4]$,[21] were prepared by utilizing published procedures. Other reagents (Fluka and Strem) were used as received, and solvents were distilled directly prior to use. CH_2Cl_2 was dried by refluxing under nitrogen over calcium hydride and redistilled directly before electrochemical measurements. Methanol was carefully treated with a small amount of sodium wire to generate sodium methoxide. This destroyed water, and pure methanol was distilled from this solution. ^{1}H NMR spectra at 20 °C were recorded on a Bruker Advance DPX 300 NMR spectrometer at 300 MHz, with chemical shifts presented as δ values referenced to $SiMe_4$ at 0.00 ppm utilizing $CDCl_3$ as the solvent. $CDCl_3$ was made acid-free by passing it through basic alumina immediately before use. UV spectra were recorded on a Cary 50 Probe UV/vis spectrophotometer. The temperature was controlled to within ±0.1 °C using a water bath. Melting points were determined with an Olympus BX 51 microscope equipped with a Linkam THMS 600 heating apparatus and are uncorrected. Elemental analysis was conducted by the Canadian Microanalytical Service, Ltd.

Rhodium Complex Synthesis. The synthesis of **3** may serve as an example. Solid β-diketone **1** (0.05 g, 0.11 mmol, 2 equiv) was added to a solution of $[Rh_2Cl_2(cod)_2]$ (0.03 g, 0.05 mmol) in DMF (2 mL). The resulting solution was stirred for 1 h, and the product precipitated with an excess of water. The precipitate was filtered off and dissolved in ether, and the organic layer was washed with water. The ether layer was dried over Na_2SO_4 and filtered, and the solvent was removed under reduced pressure. The residue was essentially clean **3** (0.06 g, 72% yield) but could be crystallized from an open flask containing a mixture of dichoromethane/hexane (1:1). Mp: 179−181 °C. ^{1}H NMR (300 MHz, $CDCl_3$)/ppm: δ_H 4.13 (4H; m; 4 cod-CH), 2.52 (4H; m; 0.5 × 4 cod-CH_2), 2.46 (6H; s; 2 × CH_3), 2.44 (3H; s; SCH_3), 2.39 (6H; m; 2 × SMe), 1.86 (4H; m; 0.5 × 4 cod-CH_2). Anal. Calcd for $C_{22}H_{27}O_2RhS_8$: C, 38.70; H, 3.99. Found: C, 38.45; H, 3.90.

Characterization Data for 4. The purification was the same as that for **3**. Yield: 78%. Mp: 202−205 °C. ^{1}H NMR (300 MHz, $CDCl_3$)/ppm: δ_H 5.46 (1H; s; CH), 4.12 (4H; m; 4 cod-CH), 2.49 (4H; m; 0.5 × 4 cod-CH_2), 2.19 (3H; s; CH_3), 2.02 (3H; s; TTF-CH_3), 1.95 (6H; s; 2 × TTF-CH_3), 1.85 (4H; m; 0.5 × 4 cod-CH_2). Anal. Calcd for $C_{21}H_{24}O_2RhS_4$: C, 46.75; H, 4.48. Found: C, 46.59; H, 4.49.

Kinetic Measurements. A computer-controlled Applied Photophysics SX.18MV stopped-flow instrument was used to collect kinetic data. Observed rate constants were determined using the associated Applied Photophysics software. The reaction

(19) (a) March, J. *Advanced Organic Chemistry*, 4th ed.; John Wiley and Sons: New York, 1992; pp 17−20, 263−269, and 273−275. (b) Auger, A.; Muller, A. J.; Swarts, J. C. *Dalton Trans.* **2007**, 3623–3633.

(20) Giordano, G.; Crabtree, R. H. In *Inorganic Synthesis*; Shriver, D. F., Ed.; Wiley: Chichester, U.K., 1979; Vol. *19*, pp 218−220.

(21) LeSuer, R. J.; Buttolph, C.; Geiger, W. E. *Anal. Chem.* **2004**, *76*, 6395–6401.

temperature was controlled to within 0.1 °C using a water bath. The UV/vis spectra of **3**, **4**, and [Rh(phen)(cod)]$^+$ were determined in methanol at 25 °C on a Cary 50 Probe UV/vis spectrophotometer. From these spectra, suitable wavelengths were determined, where the reaction was followed kinetically; see Table 1. All substitution reactions were performed in freshly distilled methanol under pseudo-first-order conditions, with phen concentrations between 40 and 500 times in excess over [Rh(β-diketonato)(cod)] = 0.55 mmol dm^{-3} for **3** and 0.067 mmol dm^{-3} for **4**. At least five different concentrations in this range were utilized for each complex. The activation enthalpy and entropy, $\Delta H^{\ddagger}$ and $\Delta S^{\ddagger}$, were obtained from kinetic runs between 5 and 41 °C, with five different temperatures employed to establish the temperature dependence for each substitution reaction.

Calculations. Reaction rates satisfy the expressions

$$\text{rate} = (k_s + k_2[\text{phen}])[\text{Rh}(\beta\text{-diketonato})(\text{cod})]$$

$$= k_{obs}[\text{Rh}(\beta\text{-diketonato})(\text{cod})] \text{ with}$$

$$k_{obs} = k_2[\text{phen}] + k_s \quad (1)$$

The experimentally determined pseudo-first-order rate constants, k_{obs}, were converted to second-order rate constants, k_2, by determining the slope of the linear plots of k_{obs} against the concentration of the incoming phen ligand according to eq 1 (Figure 2). Nonzero intercepts showed that the reaction took place to a noticeable extent via a solvent pathway with rate constant k_s.

Activation parameters were determined from the Eyring relationship, eq 2 with $\Delta H^{\ddagger}$ = activation enthalpy, $\Delta S^{\ddagger}$ = activation entropy, k = rate constant, k_B = Boltzmann's constant, T = temperature, h = Planck's constant, and R = universal gas constant.

$$\ln\frac{k_2}{T} = -\frac{\Delta H^{\ddagger}}{RT} + \frac{\Delta S^{\ddagger}}{R} + \ln\frac{k_B}{h} \quad (2)$$

The (Gibbs) free energy of activation may be calculated from $\Delta G^{\ddagger} = \Delta H^{\ddagger} - T\Delta S^{\ddagger}$.

Electrochemical Measurements. Measurements on ca. 1.0 mmol dm^{-3} solutions of **3** and **4** in dry CH_2Cl_2 containing 0.10 mol dm^{-3} [N(^{n}Bu)$_4$][B(C$_6$F$_5$)$_4$] as the supporting electrolyte were conducted under a blanket of purified argon at 25 °C utilizing a BAS 100 B/W electrochemical workstation interfaced with a personal computer. A three-electrode cell, which utilized a platinum auxiliary electrode, a glassy carbon working electrode (surface area: 0.031 cm^2), and an in-house-constructed Ag/Ag$^+$ reference electrode, was used. The working electrode was pretreated by polishing on a Buehler microcloth first with 1 μm and then $^1/_4$ μm diamond paste. The reference electrode was constructed from a silver wire inserted into a solution of 0.01 mol dm^{-3} $AgNO_3$ and 0.1 mol dm^{-3} [N(^{n}Bu)$_4$][B(C$_6$F$_5$)$_4$] in acetonitrile, in a luggin capillary with a vycor tip. This luggin capillary was inserted into a second luggin capillary with vicor tip filled with a 0.1 mol dm^{-3} [N(^{n}Bu)$_4$][B(C$_6$F$_5$)$_4$] solution in acetonitrile. Successive experiments under the same experimental conditions showed that all formal reduction and oxidation potentials were reproducible within 5 mV. All potentials in this study were experimentally referenced against the Ag/Ag$^+$ couple but were then manipulated on Excel to be referenced against Fc/Fc$^+$, as recommended by IUPAC.[22] However, because the ferrocene couple interferes with the TTF signals, each experiment was first performed in the absence of any internal standard and then repeated in the presence of <1 mmol dm^{-3} decamethylferrocene (Fc*). A separate experiment containing only ferrocene and decamethylferrocene was also performed. Data were then manipulated on a Microsoft Excel worksheet to set the formal reduction potential of the Fc/Fc$^+$ couple to 0 V. Under our conditions, the Fc*/Fc*$^+$ couple was at -607 mV vs Fc/Fc$^+$, $i_{pc}/i_{pa} = 0.99$, and $\Delta E_p = 79$ mV, while the Fc/Fc$^+$ couple itself was at 220 mV vs Ag/Ag$^+$, $i_{pc}/i_{pa} = 0.97$, and $\Delta E_p = 72$ mV.[23]

Acknowledgment. Financial assistance by the South African NRF under Grant 2054243 and the Central Research Fund of the University of the Free State is gratefully acknowledged.

Supporting Information Available: Cyclic voltammograms of **3** and **4** at different scan rates highlighting Rh^{III} reduction, a table of all electrochemical data, and the relationship between (scan rate)$^{0.5}$ and i_{pa}. This material is available free of charge via the Internet at http://pubs.acs.org.

(22) Gritzner, G.; Kuta, J. *Pure Appl. Chem.* **1984**, *56*, 461–466.

(23) A leading reference describing the electrochemical activity and behavior of ferrocene and decamethylferrocene in a multitude of organic solvents is as follows: Noviandri, I.; Brown, K. N.; Fleming, D. S.; Gulyas, P. T.; Lay, P. A.; Masters, A. F.; Phillips, L. *J. Phys. Chem. B* **1999**, *103*, 6713–6722.